視網膜影像上血管串珠疾病自動診斷系統
Automatic Diagnosis System of Venous Beading in Retinal Images

楊晴雯 馬代駿 趙順清 溫嘉憲 張建禕
Ching-Wen Yang[1] Dye-Jyun Ma[2] Shuen Ching Chao[2] Chia-Hsin Wen[1] Chein-I Chang[3]

[1]Computer Center, Taichung Veterans General Hospital, Taichung, Taiwan, ROC
[2]Department of Electrical Engineering, National Chung-Hsing University, Taichung, Taiwan, ROC
[3]Department of Electrical Engineering, University of Maryland Baltimore County Baltimore, MD 21228-5398, U. S. A.

摘要

本文提出一個鐘型比對濾波器來分割出視網膜影像上的血管,及一個視網膜影像上血管串珠疾病自動診斷系統.

Abstract

In this paper, we proposed a bell-shaped matched filter for extracting blood vessel, and an automatic diagnosis system of venous beading in retinal image. The automated detecting algorithm is performed in several steps. The vein is first extracted from the background by bell-shaped matched filter to generate a rough shape. Morphological closing algorithm is used to erase the noise in the background and to close any holes arising from noise. Morphological thinning is then applied to the binary image for finding the forks of the blood vessels. The forks must be deducted for creating the pattern of the veins without branch. Finally, a Shape Cognitron is applied to extract the feature of the vascular shape. According to the feature of the veins, the neural network technique is used to analyze the difference between venous beading veins and normal veins and to classify those veins into to categories, normal and venous beading.

1. Introduction

The *venous beading* is a powerful predictor of diabetic retinopathy, comparing to other types of retinal abnormality [1]. Accurate assessment of the degree of venous beading is particularly important so that the opportunity for treatment is not missed.

Veins exhibiting beading have diameters that do not decrease monotonically with distance from the macula. Beaded veins exhibit periodic changes in diameter along their lengths, somewhat like a string of sausages. Fig. 1 shows the typical shapes of a normal vein and a vein exhibiting beading [2,3].

Previous works on analyzing retinal images have oncentrated mainly on detecting vessels and microaneurysms. Adaptive thresholding followed by binary thinning [4] has been used for detecting vessels. A set of convolution masks [5] obtained by rotating a linear feature detector of a Gaussian cross-section was used for extracting blood vessels in retinal images. A morphological transformation of the positive image [6] was used for detection of microaneurysms, and with counting microaneurysms being used as a method for grading the severity of diabetic retinopathy. As for other techniques in retinal image processing, automated registration of retinal images [7] enables accurate comparisons between images taken at different time and provides the ability to automate the calculation of changes for both lesions and normal anatomic structure. Fluorescein angiography [8] has been an established clinical technique, which helps in the differentiation of retinal disease and can determine if laser treatment of the retina is warranted. Detection of non-prefused zone [9] in retinal image has been used for detecting and monitoring the early stages of diabetic retinopathy.

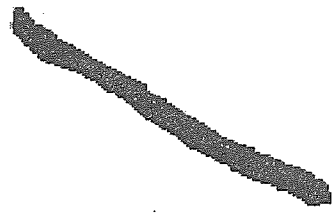

(a)

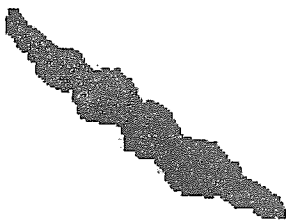

(b)

Fig. 1 Vein example. (a) A normal vein. (b) A vein exhibiting beading.

In this paper, we devote our attention to the study of automated diagnosis of the retinal disease of diabetic retinopathy. Diabetic retinopathy has great influence to the adults in the developed countries. The most serious damage to the retina may be blindness, and therefore, the prevention and tracing of diabetic retinopathy is extremely important. A specific pathology called *venous beading* has been known to be a good indicator for the degree of *diabetic retinopathy* [1]. Our goal here is thus to build an automated diagnosis system for the venous beading. Our work consists of two main parts:

1) *Extracting blood vessels of retinal image:*
Blood vessels in retinal images show enormous information about venous beading, for the disease exhibits an irregular shape of the vein like a string of sausage. The detection of blood vessels plays an important step in the automatic diagnosis process of venous beading. Here, we develop a both effective and efficient method for extracting blood vessels of retinal images. The method is based on the concept of match filter, and improves upon an existing method [5] in terms of efficiency.

2) *Automated detection of venous beading:*
To design a fully automated detection and diagnosis process for venous beading, we combine blood vessels extraction procedure of the previous part with the second part, which uses the extracted blood vessels as inputs to distinguish beaded veins from normal veins. The second part is done by *Shape Cognitron neural network* approach. Loosely speaking, the shape of the veins is first analyzed by the Shape Cognitron feature extracting process, and a neural network method is then applied to recognize beaded shape. The approach is new for retinal disease diagnosis, and the results show high effectiveness and reliability of the approach.

2. Extracting blood vessel by Bell-shaped matched filter

It was observed in [5] that these vessels almost never have ideal step edges. Although the intensity profile varies in every vessel, it may be approximated by a Gaussian curve:

$$f(x,y) = A\{1 \pm K\exp(-d^2/2\sigma^2)\} \qquad (1)$$

Where d is the perpendicular distance between the point (x, y) and the straight line passing through the center of the blood vessel in a direction along its length, σ defines the spread intensity profile, A is the gray-level intensity of local background, and K is a measure of reflectance of the blood vessel relative to its neighborhood.

The ideal behind the design of bell-shaped matched filter here is to have one single convolution mask (instead of 12) that can cover the Gaussian shape in every direction. The kernel K(x, y) is

$$K(x,y) = -\exp(-(x^2+y^2)/2\sigma^2) \qquad (2)$$

We truncate the tail at $\sqrt{u^2+v^2} = 3\sigma$. With m being mean value of kernel inside the disk of the radius of 3σ, and convolution mask of new matched filter is simply give by

$$K'(x,y) = K(x,y) - m \qquad (3)$$

Note that the new kernel has the Gaussian shape along every direction, thus making it bell- shape. To implement the *bell-shaped filter*, the coefficients of the kernel are each multiplied by a scale factor of 10 and truncated to their nearest integer. In Fig. 2, we show a typical bell-shaped kernel using σ=2.

0	0	0	0	0	0	0	2	0	0	0	0	0	0	0
0	0	0	0	2	2	2	2	2	2	2	0	0	0	0
0	0	0	2	2	1	1	1	1	1	2	2	0	0	0
0	0	2	2	1	0	-1	-1	-1	0	1	2	2	0	0
0	0	2	1	0	-1	-3	-4	-3	-1	0	1	2	0	0
0	0	2	1	-1	-3	-6	-7	-6	-3	-1	1	2	0	0
0	2	2	1	-1	-4	-7	-8	-7	-4	-1	1	2	2	0
0	0	2	1	-1	-3	-6	-7	-6	-3	-1	1	2	0	0
0	0	2	1	0	-1	-3	-4	-3	-1	0	1	2	0	0
0	0	2	2	1	0	-1	-1	-1	0	1	2	2	0	0
0	0	0	2	2	1	1	1	1	1	2	2	0	0	0
0	0	0	0	2	2	2	2	2	2	2	0	0	0	0
0	0	0	0	0	0	0	2	0	0	0	0	0	0	0

Fig. 2 A Bell Shape Mask using σ=2.

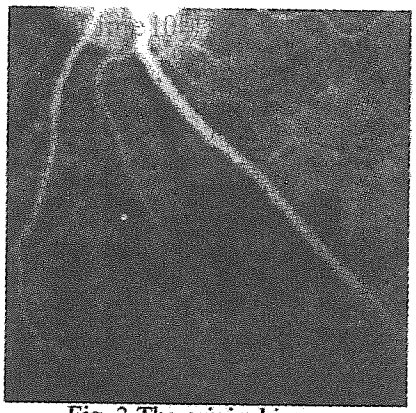

Fig. 3 The original image.

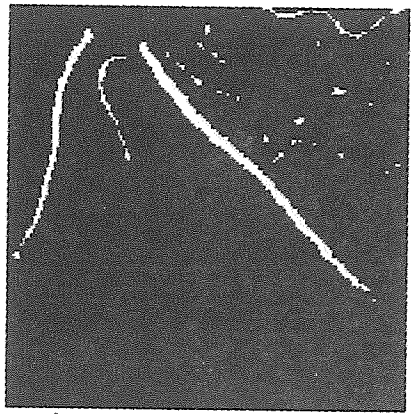

Fig. 4 After a bell-shaped filter and automated thresholding apply on Fig. 3.

It is used to roughly extract the vein shape from the background. To further extract veins from the background, some global automated thresholding schemes are used on the image. Fig. 3 shows the original retinal vein pattern,

and after applying the bell-shaped matched filter and automated thresholding scheme to the original image, the result is shown in Fig. 4.

Delete noise and morphological closing

The bell-shaped matched filter can be viewed as a combined and simplified form of Gaussian match filters. Although the results generated by the bell-shaped filter are close to those by Gaussian match filters, more noise will be generated by the bell-shaped method.

To erase the noise, a simple process is adopted in that the noise is deleted whenever its size is under 30 pixels (the threshold number may depend on the average of the noise size).

Morphological closing is used to fill any holes and smooth the edges in the binary silhouette of the veins. The morphological closing consists of a *dilation* followed by an *erosion*. Both operations are performed with the same structuring element. The size and shape of an appropriate structuring element are dependent of the image resolution, the size and shape of image feature (veins), and the size and shape of the holes to be filled. The structuring element of closing operation is shown in Fig. 5.

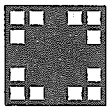

Fig. 5 Structuring element

Fig. 6 shows the result of Fig. 4 after noise delete and use of morphological closing.

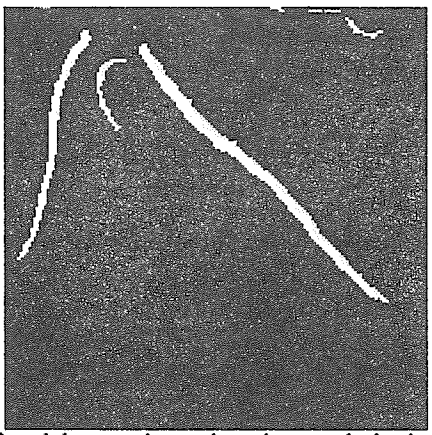

Fig. 6 After deletes noise and apply morphological closing on Fig. 4.

Elimination of branch

Because of irregular blood stream pressure, the veins' shape near the branch will be irregular which is not caused by the diabetic retinopathy. Due to this irregularity, the automated diagnostic process may mistakenly view the normal veins as the venous beading. The nonbranch vein segments are the regions to be discriminated by diagnostic systems and thus the bifurcation should be erased before the pattern can be recognized. First, we are thinning the pattern of the blood vessels with *morphological thinning algorithm* [10].

The thinning algorithm employed here uses a 3×3 pixel neighborhood centered on the pixel of interest in the morphologically closed binary image. Let C denote the gray level of the pixel of interest, eX denote the value of X direction returned from the edge function [10] which decides whether the pixel is on the edge if they have two to six neighbors, vX denotes the value of X direction, where $X \in \{E, S, W, N, SE, SW, NE, NW, C\}$. In general, the thinning strategy set C=FALSE if C is determined to be on a vein edge. More specifically, a pixel survives an iteration of the thinning algorithm if

$$vC \bullet (\overline{eC} + (eE \bullet vN \bullet vS) + (eS \bullet vW \bullet vE) + (eE \bullet eSE \bullet eS))$$

is true, where $\bullet$ and + denote logical AND and OR, respectively.

After pixels have been removed using the algorithm above, it is necessary to repeat the operation using southward bias expression, which is the same except that north and south are interchanged. After elimination of the edge element, unnecessary skeleton elements may remain which can not be removed using the algorithm above. A final clean-up phase is necessary to eliminate staircase as described in [10].

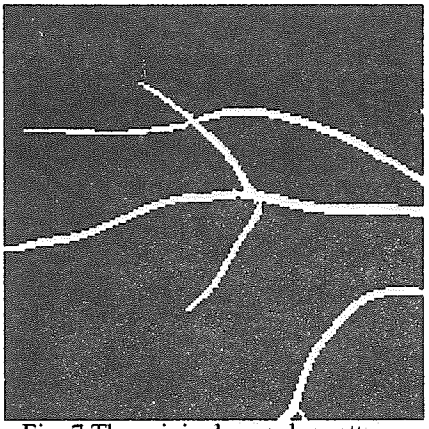

Fig. 7 The original vascular pattern.

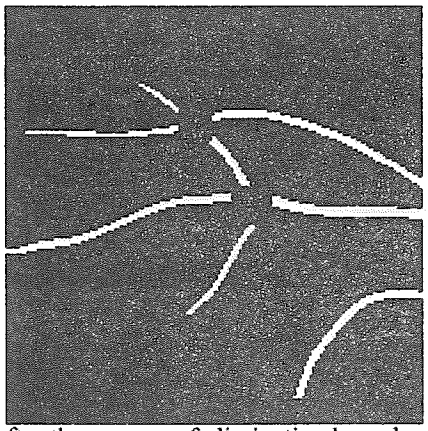

Fig. 8 After the process of eliminating branch of Fig. 7.

The thinning algorithm gives the skeleton image, from which, we can find out fork points with more than 3 neighbors as branch points. Treating each branch point as the origin and drawing a square, we can erase vascular pixels in the square. The size of the square depends on the ratio of the vascular pixels occupying in the square. After erasing the bifurcation, some small unbranch segments which may have influence on discriminating process may be created. We throw away these segments by noise delete process. The following two illustrations, Fig. 7 and Fig. 8, show the results from the above procedures.

3. Extracting the Shape Feature by Shape Cognitron

The unbranch pattern will be the input to the Shape Cognitron neural network, and the angle of every pixel in the pattern is analyzed. In the output of shape cognitron neural network [11], there are <22.5°, 45°, 90°, 135°, 180°, 225°, 270° and 360° being represented by 2, 3, 4, 5, 7, 9, b (11) and c (12), respectively. In Fig. 9, we illustrate the graphs of the boundary points with varying degrees of shape curvatures. In the 3-D figure map which is the output from the Shape Cognitron, every pixel is represented by a hexadecimal numbers from 2 to C. According to the irregular shape in venous beading, we can distinguish between venous beading and normal vein pattern by recognizing the 3-D figure map. We can then apply backpropagation neural network [12,13] in the discriminating phase.

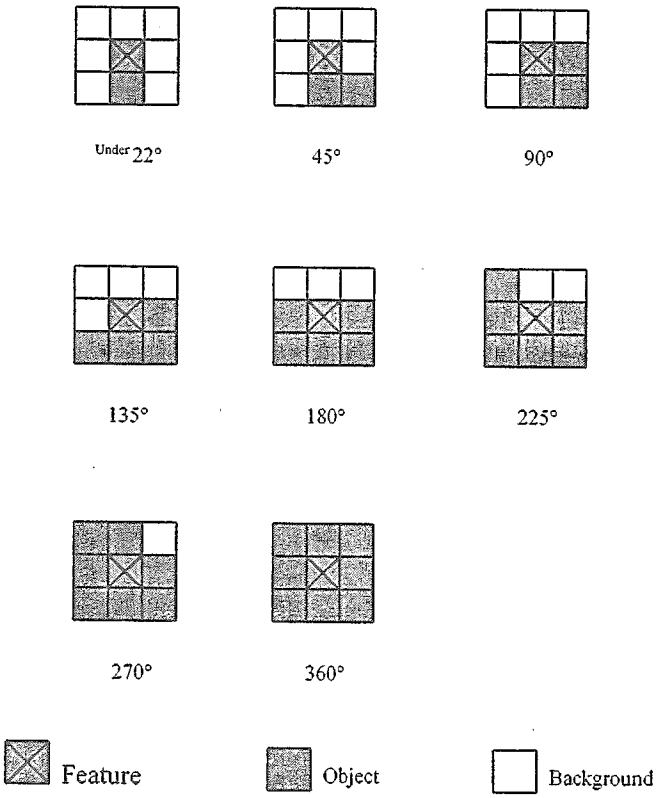

Fig. 9 The boundary points with varying degrees of shape curvatures.

Shape Cognitron Neural Network

The structure of the Shape Cognitron neural network is shown in Fig. 10.

The input layer (*U*0 layer) receives the pattern by a 20×20 cell plane Here we use the 20×20 input pattern as an example shown in Fig. 11 for illustration.

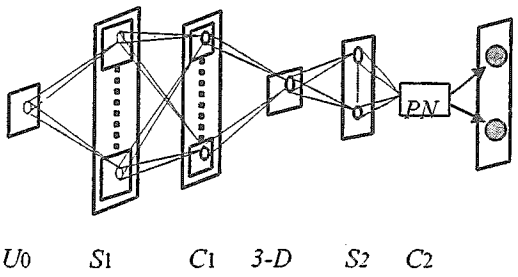

Fig. 10 The structure of the Shape Cognitron neural network.

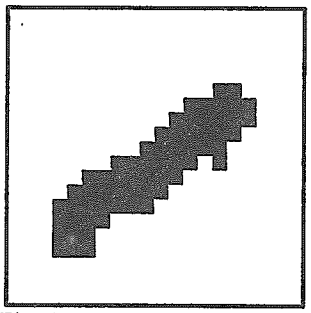

Fig. 11 Input Pattern (20×20)

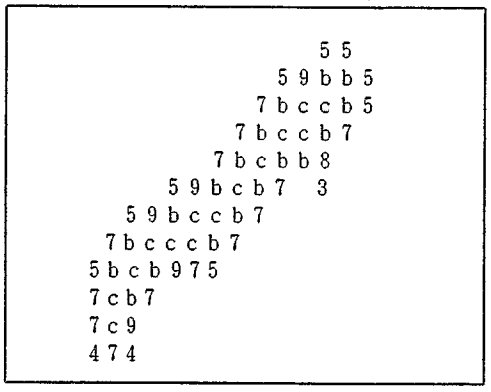

Fig. 12 A 3-D figure of the pattern in Fig. 11

Shape Curvature	Number
$<45^0$	2
45^0	3
90^0	4
135^0	5
180^0	6,7
225^0	8,9
270^0	a,b
360^0	c

Table 1 Shape curvature generated by Shape Cognitron

The $S1$ layer responds to the $U0$ layer by 20 20×20 cell planes. The $C1$ layer creates 8 20×20 cell planes by merging the 20 20×20 cell planes of the $S1$ layer.

In 3-D figure layer, there is only one 20×20 cell plane call 3-D figure map, which is generated by summing all the cell planes in $C1$ layer. The pixels of the summed cell plane will take a value ranging from 0 to 12 (C). The 3-D figure map of the pattern in Fig. 11 is shown in Fig. 12. Table 1 shows the numeric representations obtained from the 3-D figure for 8 various shape curvatures.

After generating the 3-D figure map, the $S2$ layer and $C2$ layer are responsible for recognizing venous beading. In the $S2$ layer we calculate the probabilities of some numerical symbols appearing in the 3-D figure map as the feature values (Table 2).

	Feature Name	Description
1	vein number	the number of the vascular branches
2	total perimeter	sum (2, 3, 4, 5, 7, 9)
3	total length	the total length of all vascular branches
4	irregularity degree	sum(2, 3, 4) / total perimeter
5	radian degree	sum(4, 5, 9) / total perimeter
6	smooth degree I	sum(7) / total perimeter
7	smooth degree II	sum(7 with two or more neighbor=7) total perimeter
8	avg. irregularity degree	sum(2, 3, 4) / vein numbers
9	avg. radian degree	sum(4, 5, 9) / vein numbers
10	avg. smooth degree I	sum(7) / vein numbers
11	avg. smooth degree II	sum(7 with two or more neighbor=7) total perimeter
12	'b' ratio without neighbor '7'	sum(b without neighbor=7) / sum(b)
13	the ratio of 'b' and perimeter	sum(b without neighbor=7) / total perimeter

Table 2 The feature values and it's description

The feature values will be inputted to the $C2$ layer for training and discriminating. The back propagation neural network BNN are used in the C2 layer for our diagnosis process,

4. Experiment Results

For experiment results, we use 61 512×512 grayscale retinal images, including 32 beaded images and 29 normal images, which were provided by Hsin-Chu Public Hospital. The beaded part and normal part of the images were signed by the doctor and segmented as 180×180 image patterns. Among the image patterns, we randomly take 20 patterns as training patterns, with 10 patterns of them being beaded and the other being normal.

We choose from the feature values of Table 2 to form a feature vector for recognizing venous beading. Three such vectors are formed, each of which will be individually applied for the neural network for both training and discriminating. Table 3 shows the three vectors and their correspond feature values.

Vector Set No.	Element of vector
Vector Set No. 1	4, 5, 6, 8, 9, 10, 12
Vector Set No. 2	4, 5, 7, 8, 9, 11, 13

Table 3 Three feature vectors extracting from $S2$ layer.

In the experiment, we use the 3-layer BNN structure. In input layer, input node number is the number of elements in the feature vector generated from the $S2$ layer. Table 4 shows the results of 41 test patterns recognized by BNN.

	Beaded veins patterns (22)		Normal veins patterns (19)	
Recognized result	Beading	Normal	Beading	Normal
Vector Set No. 1	19	3	4	15
Vector Set No. 2	17	5	1	18

Table 4 The recognized result by BNN

From Table 4, we can calculate recognized rates base on the three feature vectors for BNN, and the results are shown in Table 5.

	Recognized rate	
	Hit rate	Error rate
Vector Set No. 1	83%	17%
Vector Set No. 2	85%	15%

Table 5 Three feature vectors' recognized rate on BNN.

From Table 5, we observe that vector set No. 2 have a higher hit rate than the other one feature vector. Thus,

vector set No. 2 is more reliable than the other one feature vector for recognizing beaded veins. Both neural network methods perform almost equally well for the diagnosis of venous beading.

5. Conclusion and Future Research

In this paper, we have developed a technique for automated detection of venous beading in retinal images. In the preprocessing part, we have proposed a novel operator, called bell-shaped matched filter, for extracting blood vessels from retinal image. The new filter has significant improvement in computation time over a previous Gaussian matched filters, and in term of the quality of the extracted image, the bell-shaped matched filter performs almost equally well as Gaussian matched filters. The bell-shaped matched filter is an efficient and effective method for blood vessels extraction in retinal images. In the part of detecting venous beading, we apply Shape Cognitron neural networks for learning and discriminating beaded veins form normal veins. The experiment results show great reliability and promise of the approach.

There exist many interesting and challenging issues and topics for future research. For example, in the preprocessing part, since bead veins arise in only some parts (not all) of the retinal image, it may be helpful to automatic locate exactly ROI (regions of interesting). On the other hand, we have observed that the bell-shaped method may generate noise. It is thus interesting to find out some thresholding techniques [14,15,16] to extract veins more completely, when those thechniques combine with bell-shaped method. In the diagnosis part, we may consider more features for the Shape Cognitron neural network and study the impact. We can Also use the neural network method to classify venous beading into more categories such as "normal", "questionable", "define" and "advanced"; this way we can help the doctor more. Finally, in addition to Shape Cognitron neural network we may add the diameter variation of blood vessels to possibly enhance the reliability of the diagnosis process.

References

[1] Early Treatment Diabetic Retinopathy Study Group, "Fundus photographic risk factor for progression of diabetic retinopathy," *ETDRS Rep. No. 12. Ophthalmology,* Vol. 98, pp. 823-833, 1991.

[2] Diabetic Retinopathy Study Research Group. Report 7, "A modification of the Airlie House Classification of diabetic retinopathy," *Invest. Opthalmol. Visual Sci.*, Vol. 21, pp. 210, 1981.

[3] R. N. Frank, "Vascular disease of retina," *Retinal Disease—Biomedical Foundations and Clinical Management*, (M. O. M. Tso, Ed.), pp. 141-142. Lippincott, Philadelphia, 1988.

[4] M. Tanaka and K. Tanaka, "An automatic technique for fundus photograph mosaic and vascular net reconstruction," *Proc. of MEDINFO 80*, Tokyo, pp. 116-120, 1980.

[5] S. Chaudhuri, N. Chatterjee, N. Katz, M. Nelson and M. Goldbaum, "Detection of blood vessels in retinal images using two-dimensional matched filters," *IEEE Trans. Medical Imaging*, Vol. 8, pp. 263-269, 1989.

[6] J. Lay and B. Badouin, "Computer analysis of angioflourograms," *Proc. of VII Int. Conf. On Pattern Recognition*, pp. 927-929, 1984.

[7] A. V. Cideciyan, "Registration of ocular fundus images," *IEEE Engineering in Medicine and Biology*, Vol. 14, pp. 52-58, 1995.

[8] P. Nagin, B. Schwartz and G. Raymolds, "Measurement of fluorescein in angiograms of the optic disc and retina using computerized image analysis," *Ophthalmology*, Vol. 92, pp. 547-552, Apr. 1985.

[9] P. Jasiobedzki, D. Mcleod and C. J. Taylor, "Detection of non-perfused zones in retinal images," *Computer-Based Medical System: Fourth Annual IEEE Symposium*, pp. 162-169, 1991.

[10] M. Holt, A. Stewart, M. Clint and R. H. Perrott, "A improved parallel thinning algorithm," *Commun. ACM*, Vol. 30, No. 2, pp. 156-160, 1987.

[11] Pau-Choo Chung, **Ching-Wen Yang**, and Chein-I Chang, "A New Neural Network for Sharp Recognition: Sharp Cognitron", to appear on 1996 International Symposium Multi-Technology Information Processing (ISMIP'96), pp.195-200.

[12] F. J. Pineda, "Generalization of backpropagation to recurrent neural networks," *Physical Review Letters*, Vol. 59, pp. 2229-2232, 1987.

[13] D. F. Specht, "Probabilistic neural networks," *Neural Networks*, Vol. 3, pp. 109-118, 1990.

[14] **Ching-Wen Yang**, Pau-Choo Chung, and Chein-I Chang, "A Hierarchical Fast Two-Dimensional Entropic Thresholding Algorithm Using a Histogram Pyramid", **Optical Engineering**, Vol. 35, No.11, 1996, pp. 3227-3241.

[15] W T Chen, Chia-Hsin Wen, and **Ching-Wen Yang**, "A Fast two-Dimensional Entropic Thresholding Algorithm", **Pattern Recognition**, Vol. 27, No. 7, pp. 885-893.

[16] **Ching-Wen Yang**, Pau-Choo Chung, and Chein-I Chang, "A Pyramid Approach to Two-Dimensional Entropy Thresholding Algorithm", Proceeding of 1995 Workshop on Computer Application. pp. 59-64